New power module concept in PCB-embedded technology with silver sintering die attach

A. Tablati, N. Alayli, T. Youssef, O. Belnoue, L. Theolier, E. Woirgard

New power module concept in PCB-Embedded technology with silver sintering die attach

A. Tablati, N. Alayli, T. Youssef, O. Belnoue, L. Theolier, E. Woirgard

Abstract – This study deals with the reliability of a new power embedded PCB (printed circuit board) concept highly integrated into an electrical machine for aeronautical and automotive applications. The first part of this paper describes the assembly topology. The second part presents the main steps of module manufacturing using the silver sintering connection and the pre-impregnated composite fibers lamination. The third part shows the results of electrical and mechanical tests realized on this module. The purpose is to validate the design of a new assembly technology which offers an enhanced reliability based on the manufacturing time optimization, the reduction of the process steps, the module functionality and the feasibility.

1. Introduction

In the automotive industry, the trend is the significant integration of electrical solutions [1]. As a result, industries are faced with the need to provide devices, which are more integrated, more reliable and more energy efficient [1-4]. These devices should fit in a limited space in the car. This internal space limitation with increasing power density require to enhance heat dissipation to improve performance while reducing size [2].

The PCB Embedded technology can be a great solution to address these topics. In fact, it improves power module performances by optimizing interconnections and reducing size and weight towards miniaturization [1, 5]. This optimization leads to the reduction of parasitic inductance and to get a better thermal management [1, 6, 7]. An example of application chosen in this paper is the Smart Belt-driven Starter Generator. For this application, we have processed a PCB embedded technology.

Regarding the latter scenario, this study deals with the feasibility of a new power module concept containing four 100 V Si MOSFETs, ST315N10F7D8, set in parallel as a single switch, highly integrated in an electric machine 48 V/400 A while working in one hand on the decrease of volume and weight, on the other hand, the improvement of thermal management and mechanical strength of die attach. The technology is based on the integration of Si MOSFETs inside a PCB using sintering of silver paste for die attach and the pre-impregnated composite fibers lamination.

This paper will focus on the description of the process for a more robust assembly followed by electrical tests on a prototype to demonstrate its functionality while mechanical tests will demonstrate its strength.

2. PCB Embedded assembly design

The principle is the use of an insulated metal substrate (IMS) based on thick copper plate to transmit high current and optimize heat dissipation. Dice are stacked between two copper plates for embedding purpose.

The connection between the dice and the copper plate is ensured by silver sintering process. The electrical insulation is carried out by layers of pre-impregnated composite fibers laminated between these copper plates (see Fig. 1). Moreover, the dice gates are sintered to a copper foil, and the access to this copper foil is allowed thanks to Plated Through Hole vias (PTH).

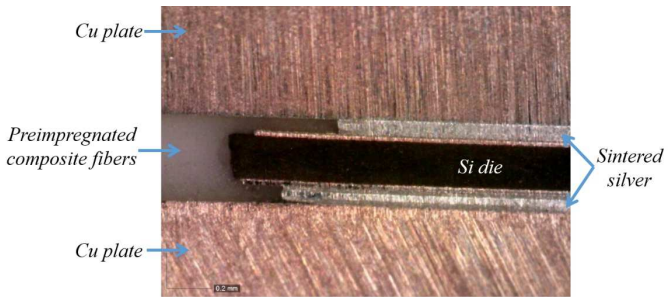

Fig. 1: Cross section view of the PCB Embedded assembly composed by a Silicon 100 V die stacked between two thick copper IMS substrates.

In the electric machine design, it is expected that the power module will be cooled down from one side, while the driver signal board will be stacked on the top of the power module. In order to ensure an excellent thermal performance, the assembly contains cavities with the thermal pads, which will be sintered near the heat source. The same pads are placed on the terminations of the module to make inter-plate interconnections in order to raise the potential of the output phase which are also shown in Fig. 2.

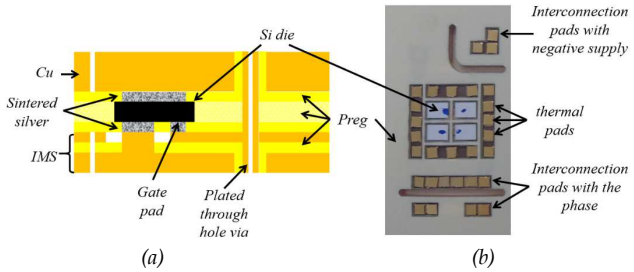

Fig. 2: (a) vertical cross-section of the PCB Embedded assembly design (b) top view of the assembly before top IMS mounting

3. PCB Embedded Process

3.1. Gate pattern deposit optimization

First the manufacturing of two copper plates panels (copper plate + preg + copper sheet) is made, based on IMS process. Each panel is milled to a depth of 70 µm, in a specific area under a group of four dice. Then two layers of preg and copper of 35 µm each, are placed in this drilling zone. The thin copper layer is used to have access to the die gate pad. Finally, all the layers are stacked and laminated to get a final 1mm thick IMS for the first panel and 1.5 mm thick IMS for the second panel.

From one hand, the gate pad is attached to the copper foil with sintered silver. On the other hand, the gate drive access is ensured thanks to PTH vias.

The screen printing is used to apply silver paste for the connection between dice pads and copper plates. This technique has already shown many advantages in electronic applications [8]. A screen for printing process of 150 µm thick was adapted, in order to deposit on very specific areas silver paste of 150 µm thick. The screen contains cavities pre-manufactured for the source, the gate and thermal pads which will be sintered near the heat sources to improve the thermal conductivity. The paste is deposited a few millimeters away from the screen cavities, this distance reduces the phenomenon of vacuum deposition between the silver paste deposit and the paste receiver panel. The deposit is made thanks to a squeegee which advances the paste in order to deposit it in the cavities.

In order to assess the deposit of the silver paste on the gate pads, which are 480 x 390 µm² wide, it was necessary to develop a screen dedicated to this manufacturing process step, the screen contains square-shaped openings with an edge ranging from 150 µm to 400 µm (with intermediate edges steps of 50 µm). Fig. 3 shows the deposits of silver paste in these openings ranging from 300 µm to 400 µm.

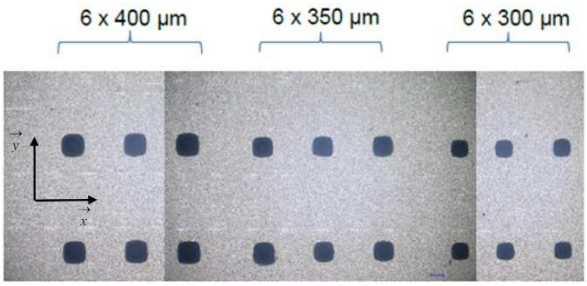

Fig. 3: Image reconstructed from a series of images of the silver paste deposit

After printing, a drying step of the silver paste is carried out to ensure the reliability of the deposit [9]. We have debinded the silver paste by drying it for 30 minutes at 130°C. Fig. 4 and Fig. 5 illustrate the result of silver paste spreading for a 200 µm screen printing sections.

Fig. 4 shows a silver paste pad extending from 200 µm to 274 µm, after debinding. It was observed that when the section varies between 150 x 150 µm² and 400 x 400 µm², this involves a paste spread of 33 %.

Fig. 5 shows the thickness profile of the silver paste pad. The thickness decreased from 150 µm to 52 µm after debinded. This thickness reduction is necessary to be taken into account in the following manufacturing steps in order to obtain undeformed copper plates.

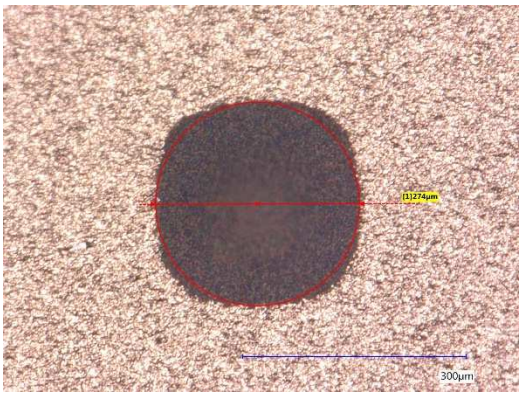

Fig. 4: Image of the increasing in silver paste spreading from 200 µm to 274 µm, after debinding

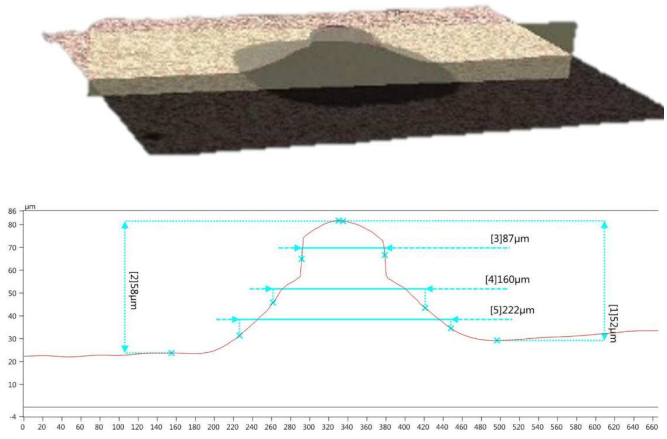

Fig. 5: a) 3D view of the silver paste deposition, b) profile of the thickness measured

A first thin pre-impregnated composite fibers sheet of 50 µm thickness, corresponding to the thickness of silver after sintering, is mounted. This sheet is necessary in order to electrically isolate the IMS substrates and compensate the thickness of silver after sintering which is 50 µm.

The dice were supplied with a standard aluminum metallization on gate and source pads, suitable with wire bonding process. In order to get a reliable die attach with sintered silver, a Ti/Au finish is deposited on these die pads. This step is followed by the placement of dice on silver area with a Pick&Place automatic machine (Datacon 2200 EVO Plus from Besi), which showed its efficiency in process time and placement accuracy [10].

Finally, a second pre-impregnated composite fibers sheet is applied. The final thickness of these pregs layers is equal to 270 µm which is the same as the die thickness.

3.2. Alignment and stacking of assembly panels

The stack is then finalized by placing the second copper plate panel on the top side. This copper plate allows to connect the positive electrode to the power module. It contains a deposit of silver paste with an area corresponding to the drain pad of the dice. Fig. 6 and Fig. 7 show this stacking.

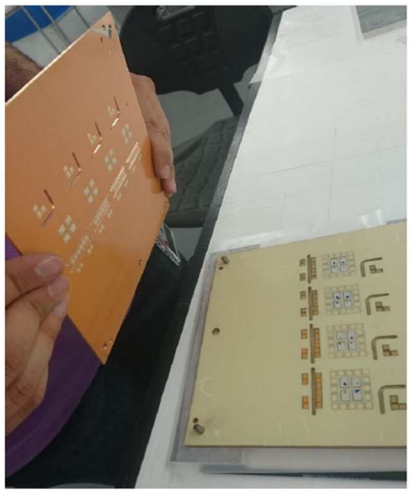

Fig. 6: Stacking of the upper plate (negative supply plane)

It is necessary to center and place with accuracy the various layers, in order to guarantee the optimization of the assembly process.

Fig. 7: Final deposition of the upper plate (negative supply plan)

3.3. Sintering Process and Stratification

The assembly, placed in a mechanical mold, is then put in the heat press « **LabPro 400 »** to realize both the pre-impregnated composite fibers lamination at a temperature of 130 °C to 135 °C and sintering the silver paste at a temperature of 195 °C achieving the attachment of dice. These parameters have been optimized according to studies on silver sintering topics [11] and pre-impregnated composite fibers formation [12]. The maximum pressure set in this apparatus is 400 kN on a 32 x 32 cm² plate. The assembly is placed on the movable low steel plate of the press showed in Fig. 8. The vacuum is set and as soon as the force exceeds the value of 64 kN, the two plates begin heating with a ramp of 10 °C/min, until the plate reaches the temperature 130 °C. From this temperature, the preimpregnated begins being stratified. A 20 min countdown begins before starting the second heating phase with a ramp of 10 °C/min until the steel plate reaches the temperature 195 °C. This temperature

corresponds to the sintering temperature of the silver paste, allowing the components attachment. The sintering phase is set for 100 min. Then, the force is released, and the heating of the plates is stopped. The assembly is cooled down to room temperature, for a minimum of 2 hours in the press.

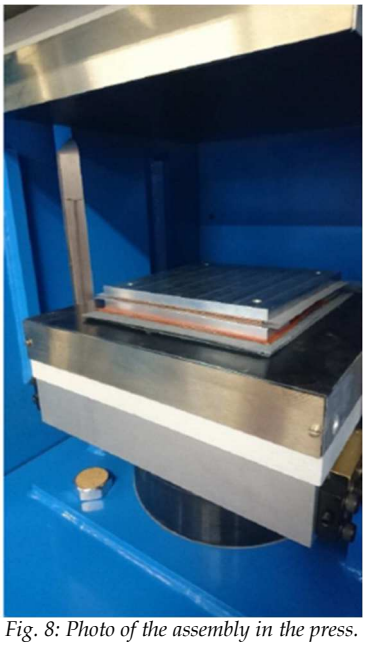

Fig. 8: Photo of the assembly in the press.

After that the assembly is removed from the mold. The creep of the preimpregnated has spread in all the cavities and on the edges of the assembly which are also shown in Fig. 9. This phenomenon makes demolding difficult.

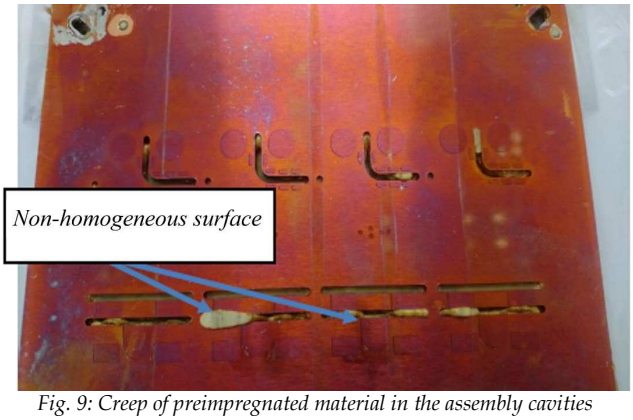

Fig. 9: Creep of preimpregnated material in the assembly cavities

This step is followed by the drilling and copper plating of PTH vias and a laser cutting of the module from copper plate. Fig. 10 shows the result of cutting the power module from the assembled copper plates. After cutting, we get a (89.3 x 29 mm²) power module, with 4.5 mm thick.

Fig. 10: Bottom view of the final module (calliper measurement in mm)

4. Process Assessment; electrical and mechanical tests

The process assembly is followed up by two ultimate tests to evaluate the functionality of the power module. The first test is mainly electrical that shows if the dice are electrically well connected and fulfill their function. The second test is mechanical and evaluates the mechanical connection of layers before reliability tests.

4.1. Electrical test

In order to investigate the behavior of embedded power MOSFET according to electrical static switching, an input voltage V_{GS} is applied between the gate and the source pads. The prototype chosen for these tests contains four 100 V Si MOSFETs, ST315N10F7D8, set in parallel as a single switch. These static characterizations are performed on a Keysight B1505A Curve Tracer, where V_{GS} varies from 0 to 10 V, by 2 V step. Thus, we measured the current-voltage output characteristic, giving the output current I_d as a function of the voltage V_{DS}, for various V_{GS}, at 25 °C.

Fig. 11 depicts the result of a good connection between PTH vias to MOSFTEs gate pad, as this curve shows a good control for embedded components. Under this pulse test, a maximum current of 340 A is reached.

According to the datasheet of the ST315N10F7D8 MOSFET used in the prototype, the on-state resistance $R_{DS(ON)-max}$ is equal to 1.75 mΩ (for V_{GS} = 10 V, I_D = 60 A). As we have 4 MOSFETs in parallel, we were expecting to have an equivalent $R_{DS(ON)-eqv} = R_{DS(ON)-max}/4$ = 0.44 mΩ. Nevertheless, according to our measure, we can deduce an on-state resistance $R_{DS(ON)}$ = 6.7 mΩ. This increase in on-state resistance value may come from a "poor" quality of silver sintering on contact surface between the dice and IMS panel.

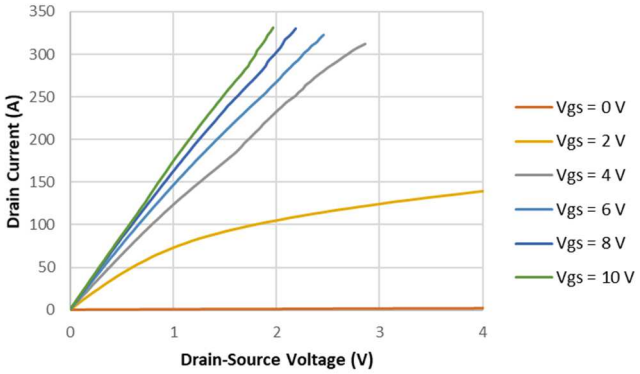

Fig. 11: Measured output characteristics of the MOSFETs embedded in parallel into the IMS PCB.

In the literature, Xu *et al.* [13] has monitored in real time the resistance of silver sintering during the process. He shows the characteristic R-t relationship. He explains the resistance change with the physical and metallurgical evolution of the silver sintering paste during process. Essential mechanisms are detected with resistance signals, including solvent evaporation, capping agent degradation and formation of first sintered clusters. The silver particles are usually covered with a capping agent to avoid low temperature sintering.

As the process solvent evaporation is performed before embedding, we may believe that the existence of capping agent increases the electrical resistance. It is difficult for free electrons to move between silver particles, leading to high value of resistance. The resistance is dominated by ions in the solvent that still imprisoned in silver layer.

Further, cross sectioning and Scanning Electron Microscopy (SEM) analysis should be performed in order to investigate this hypothesis.

4.2. Mechanical test

Fig. 12 shows the Scanning Acoustic Microscopy (C-SAM) result at 30 MHz. This figure depicts an embedded layer where sintered silver is visible on the top of Si dice that we can observe in the background. Except the top side of sintered silver, everything is encapsulated with the preg material based on fiberglass matrix. In this figure, we did not notice any void on the top side, at the interface between sintered silver and the IMS. Nevertheless, it seems that there is a sinking phenomenon of silver at the edges.

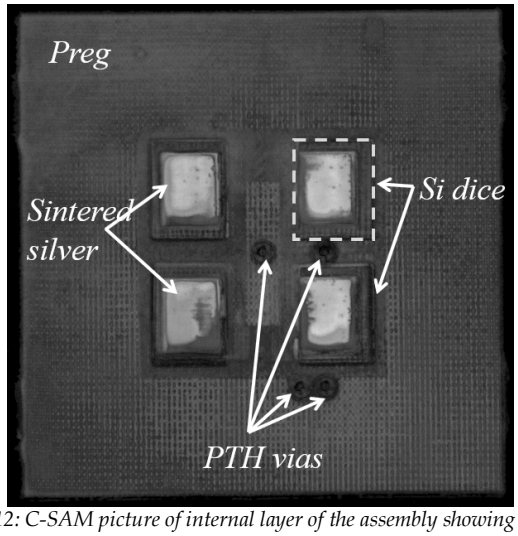

Fig. 12: C-SAM picture of internal layer of the assembly showing silver sintering materials and preg materials identified by fiberglass matrix

Then, a mechanical shear test is performed on the prototype with the help of a ROYCE 650 Universal Bond Tester. The main objective is to measure the mechanical strength of the assembly defined by the mechanical resistance of stacked material.

As the module with embedded dice has large area (25 x 25 mm²), it was not possible to perform this test on it, even with a maximum shear test force of 200 kgf, because of plastic behavior of copper.

Thereby, a shear test was performed on a nearby area (3 x 30 mm²) where two IMS are sintered together due to 6 Cu blocks and laminated on the rest of the area as shown in Fig. 13.

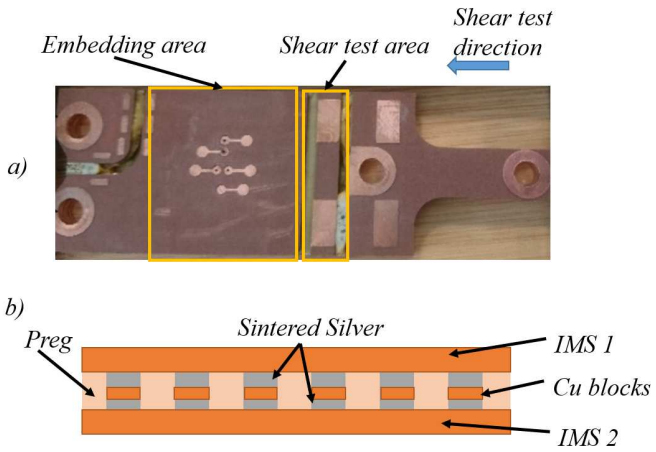

Fig. 13: Shear test area on the prototype a), with a cross view schematic of this area b).

At this level, a shear strength value of 4 MPa (~ 36 kg force) was measured. According to the standard MIL-STD-883 E (METHOD 2019.5), "all die area larger than 64 x 10^{-4} IN² shall withstand a minimum force of 2.5 kg force or a multiple thereof". In our case, the equivalent surface is 27 mm² (468 x 10^{-4} in²). With the measured shear strength; it remains greater than the standard requirements.

The fracture surfaces were analyzed with the digital microscope Keyence VHX-6000 in order to identify the type and the location of fracture. In Fig. 14, we can notice a ductile fracture with a large amount of Ag without Cu at the surface that suggests two potential failure types: a cohesive fracture in the Ag (left side) and an adhesive fracture at the Ag/IMS interface.

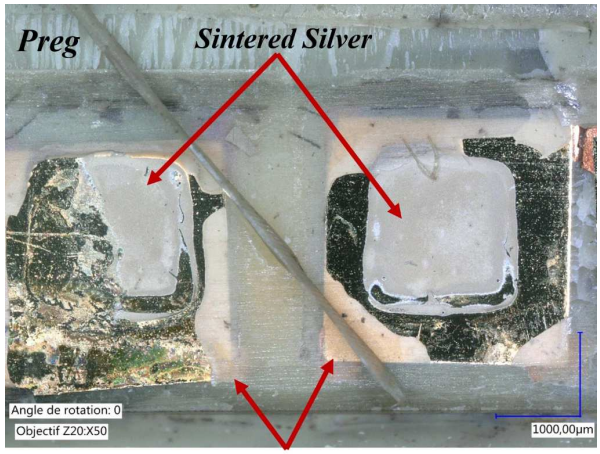

Fig. 14: Fracture picture on the Keyence digital microscope

5. Conclusions

This work has first of all illustrated a concept of a highly integrated power embedded PCB, based on optimized process, where silver sintering die connection and laminating the pre-impregnated composite fibers are performed in a single process step in order to connect the copper plates together.

Silver paste deposition was adapted for this process, in order to avoid source and gate pads short-circuit after sintering. It also highlighted experimental results obtained by a series of electrical and mechanical tests. Electrical tests show conduction and switching of the dies, while mechanical tests present high shear strength in order to demonstrate module functionality and feasibility respectively.

Further reliability tests will be performed on the power module. We believe in the reliability of silver sintering in 3D structure assembly. However, we need to identify the failure of pre-impregnated materials according to thermal ageing and thermal storage.

Declaration of competing interest

The authors declare that they have no known competing financial interests or personal relationships that could have appeared to influence the work reported in this paper.

Acknowledgements

The presented study is a part of a project, financially supported by the French National Research Agency (ANR) and a partnership agreement between VEDECOM Institute, Elvia PCB and SAFRAN Tech.

References

[1] W. Grübl, S. Gross and B. Schuch, "Embedded Components for high Temperature Automotive Applications," 2018 IEEE 68th Electronic Components and Technology Conference (ECTC), San Diego, CA, 2018, pp. 1233-1237, doi: 10.1109/ECTC.2018.00190.

[2] B. J. Hyon, Y.-S. Noh, J. S. Park, J.-H. Kim, and J.-H. Choi, "Development of High-Power Density Inverter for Automotive Applications," pp. 307–310, 2018, doi: 10.12792/iciae2018.059

[3] D. Kearney, S. Kicin, E. Bianda, A. Krivda, D. Bauman "PCB Embedded Power Electronics for Low Voltage Applications", In CIPS 2016 - 9th International Conference on Integrated Power Electronics Systems, pp. 3–8.

[4] R. Randoll, M. Asef, W. Wondrak, L. Böttcher, A. Schletz, "Characteristics and aging of PCB embedded power electronics", Microelectronics Reliability, Volume 55, Issues 9–10, 2015, Pages 1634-1639, doi: 10.1016/j.microrel.2015.06.072.

[5] F. Hou, W. Wang, T. Lin, L. Cao, G. Q. Zhang and J. A. Ferreira, "Characterization of PCB Embedded Package Materials for SiC MOSFETs", IEEE TCPMT, vol. 9, no. 6, pp. 1054-1061, June 2019, doi: 10.1109/TCPMT.2019.2904533.

[6] C. Buttay, C. Martin, F. Morel, R. Caillaud, J. Le Leslé, et al. "Application of the PCB-Embedding Technology in Power Electronics – State of the Art and Proposed Development", 3D-PEIM, Jun 2018, College Park, Maryland, United States. ff10.1109/3DPEIM.2018.8525236.

[7] Y. Pascal, M. Petit, D. Labrousse and F. Costa, "Study of a Topology of Low-Loss Magnetic Component for PCB-Embedding", 2018 7th Electronic System-Integration Technology Conference (ESTC), Dresden, 2018, pp. 1-7, doi: 10.1109/ESTC.2018.8546467

[8] D. Nakamura, "Advanced Screen Printing "Practical Approaches for Printable and Flexible Electronics "", 2008 3rd International Microsystems, Packaging, Assembly & Circuits Technology Conference, doi: 10.1109/IMPACT.2008.4783845
[9] A. Wereszczak, M. Modugno, B. Chen, W. Carty, "Contact Drying of Printed Sinterable-Silver Paste", 2017 IEEE Transactions Components, Packaging and Manufacturing Technology
[10] W. Ho & P. Ji, "An integrated scheduling problem of PCB components on sequential pick-and-place machines: Mathematical models and heuristic solutions", 2009 Expert systems in Aplications
[11] J.G. Bai, Z.Z. Zhang, J.N. Calata, G.-Q. Lu, "Low-Temperature Nanoscaled Silver as a Novel Semiconductor Device-Metallized Substrate Interconnect Material", 2006 IEEE Transactions on Components and Packaging Technologies
[12] C. Pasco & K. Kendall, "Characterization of the Thermoset Prepreg Compression Moulding Process", 2016 SPE ACCE Conference
[13] Xu, D., Kim, J.B., Hook, M.D., Jung, J.P. and Mayer, M., 2017. "Real time resistance monitoring during sintering of silver paste", Journal of Alloys and Compounds, Vol. 731, 15 January 2018, pp. 504-514.